Effect of solution temperature and cooling rate on microstructure and mechanical properties of laser solid forming Ti-6Al-4V alloy

Shuangyin Zhang (张霜银)*, Xin Lin (林 鑫), Jing Chen (陈 静), and Weidong Huang (黄卫东)

State Key Laboratory of Solidification Processing, Northwestern Polytechnical University, Xi'an 710072, China

**E-mail: shyin0925@126.com*

Received December 2, 2008

The effect of solution temperature and cooling rate on microstructure and mechanical properties of laser solid forming (LSF) Ti-6Al-4V alloy is investigated. The samples are solutions treated at 900, 950, and 1000 °C, followed by water quenching, air cooling, and furnace cooling, respectively. It is found that the cooling rate of solution treatment has a more important effect on the microstructure in comparison with the solution temperature. The martensite α' formed during water quenching results in the higher hardness and tensile strength but lower ductility of samples. With decreasing the cooling rate and increasing the solution temperature, the width of primary α laths increases, and the aspect ratio and volume fraction decrease, which make the hardness and tensile strength decrease and the ductility increase.

OCIS codes: 140.3390, 140.3590, 160.3900.

doi: 10.3788/COL20090706.0498.

In recent years, laser solid forming (LSF) of bulk near-net-shape metallic components using the solid free-form fabrication route has been shown to be a viable and promising manufacturing technology for titanium alloy parts. Especially, LSF can directly form the parts which have complex inner caves and outer shape, and is especially suitable for fabricating parts with integral rib reinforcement structures, which is the main structural characteristic of most large titanium alloy parts. A number of researches have been carried out on the LSF of titanium alloys[1−13]. Most investigations concentrated on the relationship between laser processing parameters and microstructure formation[1−5]. Wu *et al*. investigated the effect of processing parameters, such as laser power, scanning speed, powder feed rate, etc., on the microstructure of direct laser fabricated Ti-6Al-4V and burn-resistant Ti alloy[4,5]. Lin *et al*. investigated the microstructure and phase evolution in the LSF of a functionally graded Ti-Rene88DT alloy and Ti-6Al-4V-Rene88DT alloy[6,7]. Banerjee *et al*. studied the microstructural evolution and phase precipitation in a laser deposited compositionally graded Ti-V and Ti-8Al-V alloy[12,13]. As for the influence of heat treatment on microstructure and mechanical properties, Jovanović *et al*. studied the effect of annealing temperature and cooling rate on microstructure and mechanical properties of investment cast Ti-6Al-4V alloy, and showed that besides heat treatment parameters, melting and casting practice together with mold technology strongly influenced the properties of castings[14]. Gil *et al*. analyzed the effects of solution temperature and cooling rate on the Widmanstätten morphologies and mechanical properties, and investigated the mechanisms of slip and twinning involved in the plastic deformation during the cyclic straining of β-annealed Ti-6Al-4V using different cooling rates[15,16]. Zeng *et al*. investigated the effects of working process and heat treatment on the microstructural evolution and crystallographic texture of α phase in Ti-6Al-4V alloys[17].

It should be indicated that the microstructure transformation after heat treatment of LSF Ti-6Al-4V alloys has been scarcely investigated to date. In fact, compared with casted and forging samples, there should be many differences not only on microstructure and characteristic scales but also on the residual stress distribution for LSF samples due to the rapid solidification and rapid annealing repeatedly appearing during forming. This means that our understanding on the microstructural evolution and mechanical properties of titanium alloys formed by LSF is still far from complete. In particular, there is a lack of clear comprehension on the evolution of phases and microstructures during heat treatment of LSF Ti-6Al-4V alloys, which has an important influence on the final mechanical properties of LSF Ti-6Al-4V alloys.

Solution and aging treatment is the most commonly used heat treatment method of Ti-6Al-4V alloy. The important influencing factors during solution treatment are solution temperature and cooling rate, which will determine the formation of metastable phases after solution treatment, and finally affect the distribution of precipitates during aging treatment. Therefore, the aim of this work is to investigate the influence of solution temperature and cooling rate on the microstructure evolution and mechanical properties of as-deposited Ti-6Al-4V alloys.

The LSF system consisted of a 5-kW continuous-wave (CW) CO_2 laser, a four-axis numerical control working table, and a powder feeder with a lateral nozzle. The experiments were conducted inside a controlled atmosphere box, which was filled with argon gas. In the box, the oxygen content was less than 150 ppm to prevent the melt pool from oxidizing during processing, and argon gas was also used to deliver the Ti-6Al-4V powders. Gas atomized Ti-6Al-4V powders with the sizes from −100 to +150 mesh were used (Table 1). Pure titanium plates

with the thickness of 6 mm were used as substrates. In order to eliminate the moisture that was trapped in the powders, the powders were dried in a vacuum oven for 24 h. The substrate surfaces were polished with sand paper and then cleaned thoroughly with acetone prior to LSF. The processing parameters are as follows: laser power 2400−2700 W, laser spot diameters 3−5 mm, scanning velocity 4−6 mm/s, powder feeding rate 1.0−2.0 g/min, and flux of shielding gas 100−200 L/h. The dimensions of LSF samples were approximately 100×24×10 (mm).

After LSF, the samples were machined by linear cutting for further heat treatment. The dimensions of the heat treatment samples were 10 mm in length (along the laser scanning direction (X direction)), 12 mm in width (vertical to the laser scanning direction (Y direction)), and 8 mm in thickness (along Z direction). According to the heat treatment regime of Ti-6Al-4V alloys reported in Ref. [18], the samples were solution treated for 1 h at 900, 950, and 1000 °C, respectively. Three kinds of cooling methods after solution were used, i.e., water quenching (WQ), air cooling (AC), and furnace cooling (FC). The microstructures of the samples were characterized by VEGA II LMH scanning electronic microscope (SEM). The tensile tests were carried out in Instron 1196 materials testing machine.

Figure 1 shows the as-deposited sample and the typical microstructure of as-deposited Ti-6Al-4V alloys. It can be seen that there is a continuously epitaxial columnar prior-β cellular growth across several deposit layers, whose growth direction is along the deposition direction and slightly inclines towards the scanning direction. The average cellular spacing is about 300 μm. During LSF, the temperature gradient at the bottom of molten pool is very high and its direction is vertical to the laser scanning direction. Meantime, the bottom of molten pool is where solidification first initiated. For the small freezing range (about 5 K) of Ti-6Al-4V alloy, columnar to equiaxed transition is not prone to occur in most of the region in the molten pool. Thus, β-Ti columnar grains will grow epitaxially along the deposition direction. The microstructures in prior β-Ti grains consist mainly of fine Widmanstätten α-Ti laths. It also can be seen that there are several layer bands between the deposited layers, which should result from the coarsening of α-Ti laths in the heat affected zone of the deposited layers due to the reheating during the deposition of subsequent layers.

Table 1. Composition of the Ti-6Al-4V Titanium Alloy Powder (wt.-%)

H	O	N	C	Si	Fe	V	Al	Ti
0.01	0.13	0.046	≤ 0.056	≤ 0.039	≤ 0.15	4.00	6.02	Rest

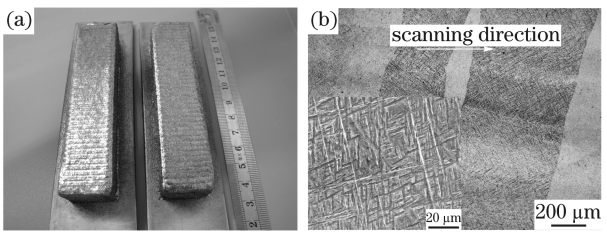

Fig. 1. (a) LSF samples of Ti-6Al-4V alloy; (b) microstructure of as-deposited Ti-6Al-4V alloy, and the inset shows a magnified part.

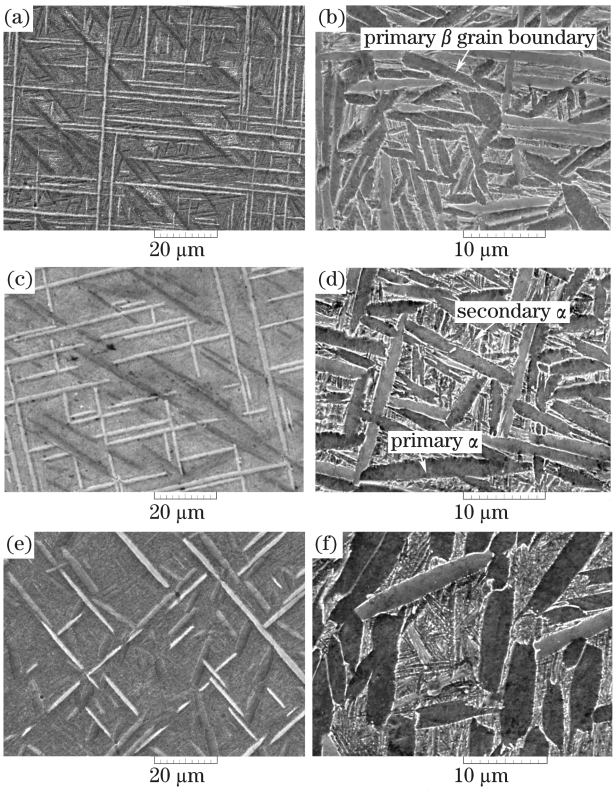

Fig. 2. SEM microstructures of LSF Ti-6Al-4V alloys treated by different cooling methods at different temperatures. (a) 900 °C, 1 h,WQ; (b) 900 °C, 1 h, AC; (c) 950 °C, 1 h, WQ; (d) 950 °C, 1 h, AC; (e) 1000 °C, 1 h,WQ; (f) 1000 °C, 1 h, AC. An aging treatment with 550 °C, 4 h, AC is performed.

Figure 2 shows the microstructures of LSF Ti-6Al-4V alloys which have been solution treated at different solution temperatures and cooling rates, respectively, prior to aging treatment (550 °C, 4 h, AC). When samples were solution treated for 1 h at 900 °C (Fig. 2(a)), 950 °C (Fig. 2(c)), and 1000 °C (Fig. 2(e)), respectively, followed by WQ and aging, the microstructures mainly consist of martensite α' and primary Widmanstätten α laths (about 1−2 μm). With increasing the solution temperature, the aspect ratio and volume fraction of primary α laths decreased and the width of α laths increased (from 1−2 μm at 900 °C to 2−3 μm at 950 °C and 3−4 μm at 1000 °C).

Figures 2(b), (d), and (f) show the microstructures of samples solution treated at 900, 950, and 1000 °C respectively for 1 h followed by AC and aging. It can be seen that the microstructure consists of basket-weave microstructure with intricately mixed multiple variants of α-Ti laths, the prior β grain boundary was decorated with the discrete α phases. With increasing the solution temperature, the aspect ratio and the volume fraction of primary α laths decreased. Meantime, the width of α laths was found to increase from 1 μm (Fig. 2(b)) with solution temperature of 900 °C to 5 μm (Fig. 2(f)) with solution temperature of 1000 °C. It can also be found that the fine secondary α laths are precipitated from retained β, whose volume fraction increases continuously

with increasing the solution temperature.

Figure 3 shows the microstructures of the samples solution treated at different temperatures for 1 h followed by FC. When the solution temperature was 900 °C, the prior β grain boundary was decorated with the continuous α phases obviously coarsened compared with that treated by AC. The basket-weave α laths were precipitated in prior β grain (Fig. 3(a)). Because the cooling rate of FC is sufficiently low, there is enough time to make α laths grow and then split and coarsen during cooling. In comparison with the microstructure with AC and aging (Fig. 2(b)), secondary α does not appear during FC, which means that secondary α should be precipitated during aging treatment for AC samples. When the solution temperature was increased to 950 °C, the width of α laths increased, the microstructure consisted of coarsening Widmanstätten α laths with a certain volume fraction of β between them (Fig. 3(b)). Segregation of vanadium or aluminum atoms in FC sample was investigated, which showed that the enrichment of α phase stabilizer aluminum in α phases and β phase stabilizer vanadium in β phases (Table 2). When the solution temperature reached 1000 °C, the microstructures consisted of equiaxed α (20−30 μm) surrounded by reticular residual β phases (Fig. 3(c)).

It can be seen from Fig. 4 that the micro hardness is remarkably affected by the cooling rate after solution treatment of as-deposited Ti-6Al-4V alloy. The hardness range of as-deposited samples was shown as shadow region. The hardness increased with increasing the cooling rate. For the same solution temperature, WQ samples have the highest hardness and present an increase of

Table 2. EDS Micro-Area Composition Analysis of Samples Treated by 950 °C, 1 h, FC for Test Positions Shown in Fig. 3(b) (wt.-%)

Position	Aluminum	Vanadium	Titanium
A	3.16	15.89	80.95
B	7.12	1.30	91.58
C	6.85	1.61	92.13

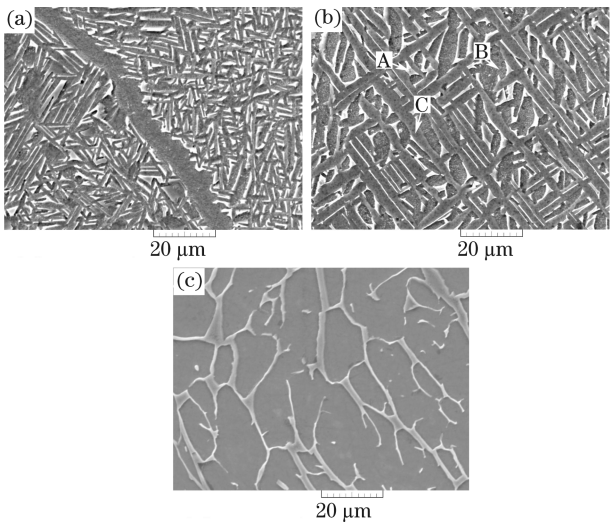

Fig. 3. SEM microstructures of LSF Ti-6Al-4V alloys treated by FC for 1 h at different temperatures of (a) 900 °C, (b) 950 °C, and (c) 1000 °C.

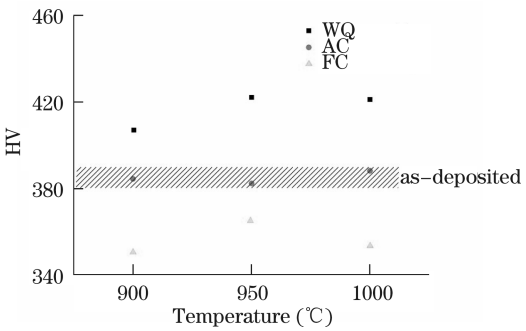

Fig. 4. Micro hardness of LSF Ti-6Al-4V alloys.

7.8% as compared with that of the as-deposited one (average HV386.72), because the martensite α' appears for WQ samples. FC samples have the lowest hardness, which is attributed to the formation of the coarsening α laths for FC samples, especially of the equiaxed α for samples solution treated at 1000 °C followed by FC. As for the influence of solution temperature, it can be seen that with increasing the solution temperature, the micro hardness of WQ samples increases and the micro hardness of the FC samples increases first and then decreases, however, the micro hardness of AC samples changes little. The influence of solution temperature on hardness is weaker than the influence of the cooling rate, which should be attributed to the significant difference in the microstructure characteristic under different cooling rates. The micro hardness of WQ samples depends on the volume fraction of martensite α' and the characteristics of primary α laths only have auxiliary effect. The micro hardness of AC samples mainly depends on the volume fraction and sizes of primary and secondary α. As for FC samples, the morphological characteristic of the primary α has an important effect on the micro hardness. For the same cooling method, the variation of solution temperature only results in a certain change of volume fractions and sizes of the composition phases.

Figure 5 shows the room-temperature mechanical properties of the samples with different solution temperatures and cooling methods. Similar to the micro hardness, WQ samples have the highest tensile strength with the same solution temperature, which have an increase of 10% as compared with that of the as-deposited one, but their ductility is the lowest. AC samples show a good combination of tensile strength and ductility, especially the significant improvement of the reduction of area. Both the tensile strength and ductility of FC samples are lower compared with AC samples due to the formation of high volume fraction of coarsening α phases during FC treatment. It is interesting to note that the ductility of the samples with solution treatment above the β transus temperature of ∼980 °C is lower than the samples solution treated below β transus temperature. Microstructure observation has shown that the martensite α' formed during WQ results in the higher hardness and tensile strength but lower ductility. With decreasing the cooling rate and increasing the solution temperature, the width of primary α lath increases, the aspect ratio and volume fraction of primary α decrease, which make the hardness and tensile strength decrease and the ductility increase.

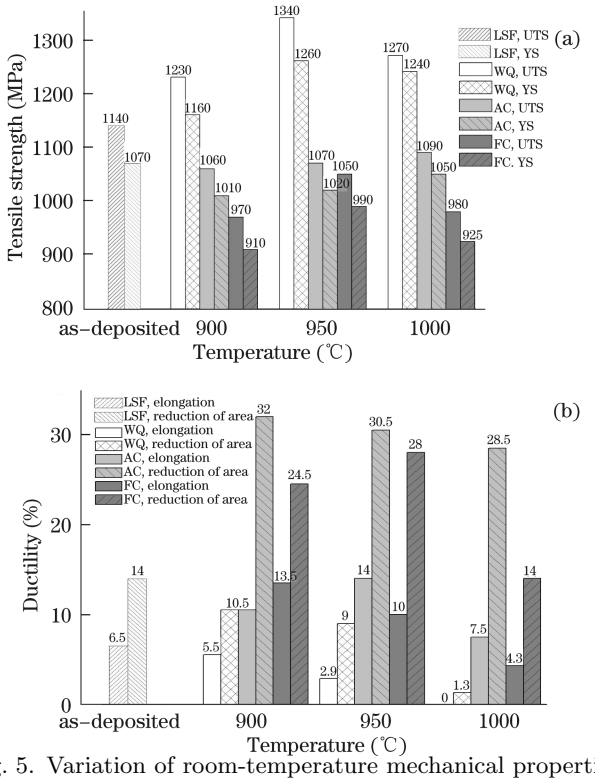

Fig. 5. Variation of room-temperature mechanical properties with the solution temperature and cooling method. (a) Tensile strength, (b) ductility. UTS and YS stand for ultimate tensile strength and yield strength, respectively.

In conclusion, the microstructure evolution during heat treatment of LSF Ti-6Al-4V alloy is investigated. The effects of solution temperature and cooling method on the microstructure and mechanical properties are analyzed. The WQ process leads to the formation of martensite α' and Widmanstätten α laths (1−2 μm). AC caused coarsening basket-weave microstructure with intricately mixed multiple variants of primary α-Ti laths (2−5 μm) and fine secondary α laths. After FC, the microstructures consist of obvious coarsening $\alpha+\beta$ laths (4−6 μm), and when the solution temperature reaches 1000 °C, the microstructures consist of equiaxed α (20−30 μm) surrounded by reticular residual β phases. The martensite α' formed during WQ results in the higher hardness and tensile strength but lower ductility. With decreasing the cooling rate and increasing the solution temperature, the width of primary α lath increases, the aspect ratio and volume fraction of primary α decrease, which make the hardness and tensile strength decrease and the ductility increase. To obtain good integrated mechanical properties for LSF Ti-6Al-4V alloys, it is suggested that the solution treatment is performed with the temperature below the β transus temperature using AC.

This work was supported by the Program for New Century Excellent Talents in University of China (No. NCET-06-0879), the National Natural Science Foundation of China (No. 50331010), the National "863" Program of China (No. 2006AA03Z0449), the National "973" Program of China (No. 2007CB613800), and the Programme of Introducing Talents of Discipline to Universities (No. 08040).

References

1. P. A. Kobryn, E. H. Moore, and S. L. Semiatin, Scripta Mater. **43,** 299 (2000).
2. K. Zhang, We Liu, and X. Shang, Opt. Laser Technol. **39,** 549 (2007).
3. S. M. Kelly and S. L. Kampe, Metall. Mater. Trans. A **35,** 1861 (2004).
4. X. Wu, R. Sharman, J. Mei, and W. Voice, Materials and Design **25,** 103 (2004).
5. X. Wu, J. Liang, J. Mei, C. Mitchell, P. S. Goodwin, and W. Voice, Materials and Design **25,** 137 (2004).
6. X. Lin, T. M. Yue, H. O. Yang, and W. D. Huang, Acta Mater. **54,** 1901 (2006).
7. X. Lin, T. M. Yue, H. O. Yang, and W. D. Huang, Metallurg. Mater. Trans. A **38,** 127 (2007).
8. J. Yu, J. Chen, H. Tan, and W. Huang, Chinese J. Lasers (in Chinese) **34,** 1014 (2007).
9. Y. Huang, Y. Yang, G. Wei, W. Shi, and Y. Li, Chin. Opt. Lett. **6,** 356 (2008).
10. J. Chen, H. Tan, H. Yang, Z. Liu, and W. Huang, Chinese J. Lasers (in Chinese) **34,** 442 (2007).
11. J. Chen, S. Zhang, L. Xue, H. Yang, X. Lin, and W. Huang, Rare Metal Mater. Eng. (in Chinese) **36,** 475 (2007).
12. R. Banerjee, P. C. Collins, D. Bhattacharyya, S. Banerjee, and H. L. Fraser, Acta Mater. **51,** 3277 (2003).
13. R. Banerjee, D. Bhattacharyya, P. C. Collins, G. B. Viswanathan, and H. L. Fraser, Acta Mater. **52,** 377 (2004).
14. M. T. Jovanović, S. Tadić, S. Zec, Z. Mišković, and I. Bobić, Materials and Design **27,** 192 (2006).
15. F. J. Gil, J. M. Manero, M. P. Ginebra, and J. A. Planell, Mater. Sci. Eng. A **349,** 150 (2003).
16. F. J. Gil, M. P. Ginebra, J. M. Manero, and J. A. Planell, J. Alloys Compounds **329,** 142 (2001).
17. L. Zeng and T. R. Bieler, Mater. Sci. Eng. A **392,** 403 (2005).
18. Editor Committee of Engineering Material Application Manual, *Engineering Material Application Manual* (in Chinese) (2nd edn.) (Standards Press of China, Beijing, 2001) pp.104−105.